Journal of Hepatocellular Carcinoma

Dovepress

open access to scientific and medical research

Open Access Full Text Article

ORIGINAL RESEARCH

Prediction of Microvascular Invasion and Recurrence After Curative Resection of LI-RADS Category 5 Hepatocellular Carcinoma on Gd-BOPTA Enhanced MRI

Juan Zhang[1,*], Yinqiao Li[1,2,*], Jinju Xia[1], Xingpeng Pan[1], Lun Lu[1], Jiazhao Fu[3], Ningyang Jia[1]

[1]Department of Radiology, Eastern Hepatobiliary Surgery Hospital, Third Affiliated Hospital of Naval Medical University, Shanghai, China; [2]School of Health Science and Engineering, University of Shanghai for Science and Technology, Shanghai, China; [3]Department of Organ Transplantation, Changhai Hospital, First Affiliated Hospital of Naval Medical University, Shanghai, China

*These authors contributed equally to this work

Correspondence: Jiazhao Fu; Ningyang Jia, Email fujiazhao@126.com; ningyangjia@163.com

Objective: This study aims to investigate the predictive value of Gadobenate dimeglumine (Gd-BOPTA) enhanced MRI features on microvascular invasion (MVI) and recurrence in patients with Liver Imaging Reporting and Data System (LI-RADS) category 5 hepatocellular carcinoma (HCC).

Methods: A total of 132 patients with LI-RADS category 5 HCC who underwent curative resection and Gd-BOPTA enhanced MRI at our hospital between January 2016 and December 2018 were retrospectively analyzed. Qualitative evaluation based on LI-RADS v2018 imaging features was performed. Logistic regression analyses were conducted to assess the predictive significance of these features for MVI, and the Cox proportional hazards model was used to identify postoperative risk factors of recurrence. The recurrence-free survival (RFS) was analyzed by using the Kaplan–Meier curve and Log rank test.

Results: Multivariate logistic regression analysis identified that corona enhancement (odds ratio [OR] = 3.217; $p < 0.001$), internal arteries (OR = 4.147; $p = 0.004$), and peritumoral hypointensity on hepatobiliary phase (HBP) (OR = 5.165; $p < 0.001$) were significantly associated with MVI. Among the 132 patients with LR-5 HCC, 62 patients experienced postoperative recurrence. Multivariate Cox regression analysis showed that mosaic architecture (hazard ratio [HR] = 1.982; $p = 0.014$), corona enhancement (HR = 1.783; $p = 0.039$), and peritumoral hypointensity on HBP (HR = 2.130; $p = 0.009$) were risk factors for poor RFS.

Conclusion: MRI features based on Gd-BOPTA can be noninvasively and effectively predict MVI and recurrence of LR-5 HCC patients.

Keywords: hepatocellular carcinoma, magnetic resonance imaging, microvascular invasion, prognosis

Introduction

Hepatocellular carcinoma (HCC) is the most prevalent type of primary liver cancer, ranking third among all cancer-related death globally.[1] Hepatic resection remains the most effective treatment option among the recommended treatment options for HCC patients. However, the 5-year postoperative recurrence rate is as high as 50%–70%,[2] and the 5-year disease-free survival rate remains low.[3]

Microvascular invasion (MVI), typically characterized by the microscopic detection of cancer cell nests within endothelium-lined blood vessels, serves as a significant predictor of post-surgical recurrence and overall poor survival in HCC patients.[4–7] Prior research has suggested that surgical resection and radiofrequency ablation should be accompanied by wider resection margin, and liver transplantation should also be considered as a potential treatment option for

Received: 19 March 2024
Accepted: 17 May 2024
Published: 25 May 2024

HCC patients with MVI.[8] Therefore, the early and accurate prediction of MVI in HCC patients may optimize patient management and improve prognosis. Nevertheless, MVI can only be confirmed through histopathologically.

Attempts to detect MVI in hepatocellular carcinoma using imaging methods have been ongoing. A number of studies have reported various MRI features that may predict MVI, including non-smooth tumor margin,[7,9–11] rim arterial enhancement,[12,13] arterial peritumoral enhancement,[7,14] and peritumoral hypointensity on hepatobiliary phase (HBP).[7,9,11,13] However, these MRI findings remain controversial, and several models constructed from MRI features lack reliability and reproducibility. Gadobenate dimeglumine (Gd-BOPTA) is distributed in the extracellular space and specifically taken up by hepatocytes,[13] thus it is applied as a hepatobiliary-specific contrast agent for clinical examination.

The Liver Imaging Reporting and Data System (LIRDS) is a liver imaging examination specification and diagnostic classification system that provides a detailed introduction and standardized requirements for imaging examination techniques, sign description terminology, diagnostic reporting, and data collection for high-risk populations with HCC.[15] Although it has been previously reported in the literature that LR-5 has a significantly better prognosis than L-M,[16] LR-5 also exhibits different clinical outcomes due to tumor heterogeneity. Not all LR-5 HCCs are amenable to surgical resection. Given the widespread clinical application of the LI-RADS system, predicting MVI and recurrence in patients with LR-5 HCC is crucial for precise patient treatment and prognostic assessment. However, the utility of Gd-BOPTA-enhanced MRI standardized imaging features as defined by LI-RADS in predicting MVI and recurrence-free survival (RFS) in LR-5 HCC patients has not been previously investigated.

The present study therefore aimed to explore the role of preoperative Gd-BOPTA-enhanced MRI features for prediction of MVI and recurrence in patients with LR-5 HCC after curative resection.

Materials and Methods

Patients

This retrospective study was approved by the Ethics Committee of the Third Affiliated Hospital of Naval Medical University. The requirement for informed consent was waived because our study was a retrospective analysis that did not involve any active patient participation or intervention in patient therapy. The data utilized were anonymized and retrospectively collected, which meant that the patients' identities were not disclosed, and there was no potential for harm or breach of privacy. This study adhered to the principles of the Declaration of Helsinki. The study population was derived from a consecutive series of 242 high-risk patients suspected of HCC (patients with cirrhosis or chronic hepatitis B virus infection) who underwent Gd-BOPTA enhanced MRI within 2 weeks before curative resection between January 2016 and December 2018. The exclusion criteria are as follows: (1) pathology confirmed non-HCC diagnosis, such as intracholangiocarcinoma, combined hepatocellular carcinoma-cholangiocarcinoma, or other metastasis tumor; (2) presence of LR-TIV; (3) not LR-5 manifestation; (4) history of treatment; and (5) follow-up period less than 1 year after curative resection. As a result, the study population ultimately comprised 132 patients with pathologically confirmed diagnosis of LR-5 HCC (Figure 1).

MRI Examination

All MRI examinations were performed using a GE Optima MR360 1.5 T system (Optima MR360, GE Healthcare, USA) equipped with an eight-channel abdominal coil. Prior to the scan, all patients were fasting for 4 hours. The unenhanced MRI protocol routinely included axial in-phase and opposed-phase T1-weighted image, axial fat-suppressed T2-weighted image, and diffusion weighted imaging (DWI) with b values of 0 and 600 s/mm.[2] After injection of the contrast agent, the arterial phase (AP), portal venous phase, and delayed phase (DP) scans were performed for 20–30, 50–60, and 90–120 seconds, respectively. Additional hepatobiliary phase (HBP) images were obtained 60 min after contrast injection. The contrast agent Gd-BOPTA (MultiHance, Bracco Inc.) was administered using a high-pressure syringe at a dosage of 0.1 mL/kg with at a rate of 2.0 mL/second, followed by rinsing with 20 mL of 0.9% sterile saline. The detailed MRI sequences are presented in Table 1.

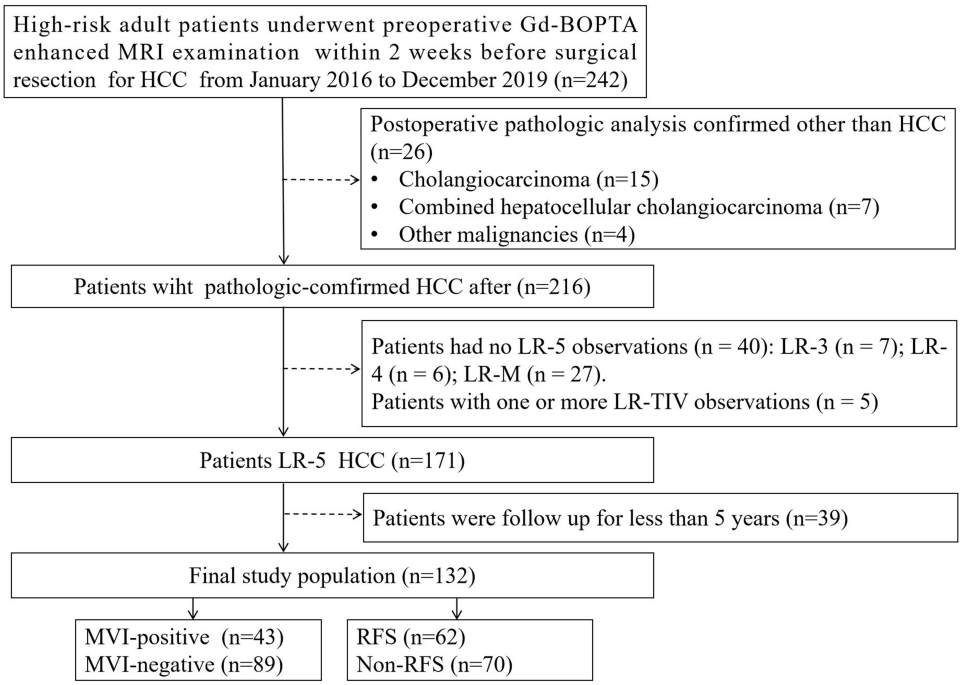

Figure 1 Flowchart of the study population.

Imaging Analysis

All MR images were independently analyzed by two radiologists (ZJ and PXP, with 8 and 18 years of abdominal imaging experience, respectively) who were unaware of the clinicopathologic and follow-up outcome. Based on the LI-RADS v2018 criteria,[15] the radiologists reached a consensus for patients at risk of HCC. HCC-related imaging features, as specified in the LI-RADS 2018 version, include major features like non-rim arterial-phase hyperenhancement (APHE), non-peripheral washout, enhancing capsule, and tumor size. Additionally, there are ancillary features like nodule-in-nodule architecture, mosaic architecture, fat in mass, blood products, corona enhancement, restricted diffusion, and mild-moderate T2 hyperintensity. Moreover, three non-LI-RADS features were considered: non-smooth tumor margin, internal arteries, and peritumoral hypointensity on HBP. Non-smooth tumor margin is defined as a bud-like projection of the tumor margin into the liver parenchyma.[17] Internal artery is a dilated artery traversing the mass in the arterial phase. Peritumoral hypointensity on HBP is characterized by a wedge- or flame-shaped area of hypointensity beyond the tumor edge in the hepatobiliary phase.[18]

Clinical Data and Histopathology Analysis

The clinical data were collected from the electronic medical record system, encompassing information on gender, age, and preoperative laboratory indices such as HBsAg, HBeAg, alpha-fetoprotein (AFP), protein induced by vitamin

Table 1 Detailed Sequences and Parameters of Gd-BOPTA Enhanced MRI

Sequences	TR/TE (msec)	FOV (mm)	Flip Angle	Thickness (mm)	Matrix
T1WI	190/4.3(2)	420 × 420	80	6	256 × 160
T2WI	6667/85	420 × 420	160	6	320 × 224
DCE	3.7/1.7	420 × 420	15	2.5	256 × 192
HBP	3.7/1.7	420 × 420	15	2.5	256 × 192
2D MRCP	4000/847	320 × 320	160	50	320 × 256

Abbreviations: DCE, dynamic contrast-enhanced; HBP, hepatobiliary phase.

K absence/antagonist-II (PIVKA-II), alanine transaminase, aspartate aminotransferase, gamma-glutamyl transpeptidase, alkaline phosphatase, total bilirubin, direct bilirubin, and albumin.

All postoperative specimens were evaluated by an abdominal pathologist with more than 10 years of experience. Microvascular invasion (MVI) was defined as the presence of cancer cells within the lumen of a microvessel composed of endothelial cells, which are only visible on microscopy. The specimens were then divided into MVI-positive and MVI-negative groups.

Follow-Up and Study Endpoint

The primary endpoint of this study was recurrence. Patients were followed up 1 month after curative surgery, every 3 months within 2 years, and annually thereafter with serum alpha-fetoprotein test and imaging examinations (contrast-enhanced ultrasound, CT, or MRI). The date of surgery, recurrence, metastasis, or last follow-up were recorded to calculate RFS. The diagnostic criteria for recurrence were positive findings on imaging examination and persistently elevated postoperative AFP levels. The follow-up deadline was February 2023.

Statistical Analysis

All statistical analyses were conducted using the SPSS software (version 26.0; IBM) and R software (version 3.6.1). Continuous variables were compared using Student's *t*-test or the Mann–Whitney *U*-test. Categorical variables were analyzed using the $\chi 2$ test. Univariate and multivariate logistic regression was performed to determine independent risk factors for MVI. The Cox proportional hazards model was used to assess potential predictors for recurrence. Survival analysis was performed using the Kaplan–Meier method and compared using the Log rank test. Differences with p-values <0.05 were considered statistically significant. Additionally, the performance of the predictors for MVI was evaluated by the area under the curve (AUC) in a receiver operating character, and concordance index (C-index) was used to assess the predictive ability of recurrence. Sensitivity, specificity, and accuracy were calculated, respectively.

Results

Clinicopathological Features of Patients

A total of 132 patients (mean age: 55.5 ± 10.9 years, 110 male and 22 female patients) with surgically confirmed LR-5 HCC were included in this study. Table 2 summarizes the clinicopathologic characteristics of LR-5 HCC in patients with or without MVI and recurrence. Among the patients, 43 (32.6%) patients were with MVI-positive, and 62 patients (47%) experienced postoperative recurrence.

Predictive Factors of MVI

Table 3 presents the result of univariate and multivariate logistic analyses for predicting MVI in patients with LR-5 HCC. Univariate logistic regression analysis indicated that mosaic architecture, corona enhancement, non-smooth tumor margin, internal arteries, and peritumoral hypointensity on HBP were significantly more prevalent in the MVI-positive group compared to the negative group. Multivariate analysis identified corona enhancement (odds ratio [OR]=3.217; 95% CI: 1.326, 7.861; $p < 0.001$), internal arteries (OR = 4.147; 95% CI: 1.596, 10.880; $p = 0.004$), and peritumoral hypointensity on HBP (OR = 5.165; 95% CI: 2.064, 12.923; $p < 0.001$) as independent predictors for MVI in patients with LR-5 HCC.

Analysis of RFS in LR-5 HCC Patients

The median follow-up time for 132 patients was 41 months (1.0–74 months). During the follow-up period, 62 patients (47%) experienced recurrence events. The 1-year, 3-year, and 5-year RFS rates for all patients were 80%, 64%, and 52%, respectively.

Predictive Factors of Recurrence

Univariate Cox regression analysis found that tumor size >5cm, multiple tumors, nodule-in-nodule architecture, mosaic architecture, corona enhancement, internal arteries, and peritumoral hypointensity on HBP were risk factors for

Table 2 Clinicopathologic Characteristics of the Study Population

Characteristic	Total (n=132)	MVI Positive (n=43)	MVI Negative (n=89)	p value	Recurrence (n=62)	Non-recurrence (n=70)	p value
Age (years)	55.5 ± 10.9	56.2 ± 10.7	55.1 ± 11.0	0.602	57.2 ± 10.5	53.9 ± 11.1	0.078
Gender				0.561			0.876
Male	110 (83.3)	37 (86)	73 (82)		52 (83.9)	58 (82.9)	
Female	22 (16.7)	6 (14)	16 (18)		10 (16.1)	12 (17.1)	
HBsAg				0.790			0.244
Absent	20 (15.2)	6 (14)	14 (15.7)		7 (11.3)	13 (18.6)	
Present	112 (84.8)	37 (86)	75 (84.3)		55 (88.7)	57 (81.4)	
Cirrhosis				0.293			**0.036**
Absent	48 (36.4)	17 (39.5)	27 (30.3)		15 (24.2)	29 (41.4)	
Present	84 (63.6)	26 (60.5)	62 (69.7)		47 (75.8)	41 (58.6)	
Serum AFP level				0.357			0.124
≤20 ng/mL	69 (52.3)	20 (46.5)	49 (55.1)		28 (45.2)	41 (58.6)	
>20 ng/mL	63 (47.7)	23 (53.5)	40 (44.9)		34 (54.8)	29 (41.4)	
Serum PT level	12.1 ± 1.0	12.0 ± 0.7	12.1 ± 1.1	0.540	12.3 ± 1.0	11.9 ± 1.0	0.069
Serum ALT level	27 (19, 39)	30 (20.7, 55.3)	27 (19, 38)	0.208	29 (19.5, 40)	27 (19, 39)	0.421
Serum AST level	27 (20, 35)	30.5 (23, 45)	26 (19, 32.5)	**0.014**	29 (21, 36)	25 (19, 33.3)	0.096
Serum GGT level	44 (26, 99)	53 (30.8, 110.5)	42 (24, 72)	0.076	49 (29.5, 109)	36 (24, 77)	**0.049**
Serum ALB level	42.3 (39.5, 45.1)	41.7 (39.6, 44.5)	42.8 (39.4, 45.5)	0.490	42.6 (39.2, 45.2)	42.6 (39.2, 45.2)	0.749
Serum pro-ALB level	213 (168.8, 271)	200 (169, 250)	217 (166, 277)	0.457	185 (155.5, 247)	232.5 (188.8, 285)	**0.003**
Serum TBiL level	13.7 (11.3, 18)	12.7 (9.0, 18.8)	14.3 (12.0, 17.6)	0.148	14.5 (12.0, 18.3)	13.4 (11.2, 17.6)	0.390
Serum dBiL level	5.1 (4.0, 6.9)	4.8 (3.5, 6.9)	5.3 (4.2, 6.7)	0.315	5.7 (3.9, 6.8)	5.1 (4.1, 6.9)	0.588
Edmondson-Steiner grade				0.529			0.146
I–II	19 (14.4)	5 (11.6)	14 (15.7)		6 (9.7)	13 (18.6)	
III–IV	113 (85.6)	38 (88.4)	75 (84.3)		56 (90.3)	57 (81.4)	

Note: p < 0.05 was defined as statistical significance (bold).

Abbreviations: AFP, alpha-fetoprotein; PT, prothrombin time; ALT, alanine transaminase; AST, aspartate transaminase; GGT, γ-glutamyl transpeptidase; ALB, albumin; pro-ALB, pro-albumin; Tbil, total bilirubin; dTbil, direct bilirubin.

Table 3 Univariate and Multivariate Logistic Analyses for MVI with Patients of LR-5 HCC

Characteristic	Univariate Analysis			Multivariate Analysis		
	OR	95% CI	p value	OR	95% CI	p value
Tumor size >5cm	1.919	0.872, 4.222	0.105			
Multiple tumors	1.027	0.029, 4.603	0.972			
LI-RADS major features						
Non-rim arterial phase hyperenhancement						
Non-peripheral washout	2.500	0.283, 22.088	0.410			
Enhancing capsule	1.048	0.489, 2.245	0.904			
LI-RADS ancillary features (favoring HCC in particular)						
Non-enhancing capsule	1.536	0.410, 4.360	0.420			
Nodule-in-nodule architecture	0.600	0.204, 1.764	0.354			
Mosaic architecture	2.837	1.328, 6.063	**0.007**			
Fat in mass, more than adjacent liver	0.716	0.276, 1.862	0.494			
Blood products in mass	2.149	0.833, 5.546	0.114			
LI-RADS ancillary features (favoring malignancy, not HCC in particular)						
Hepatobiliary phase hypointensity	0.646	0.311, 1.345	0.243			
Mild-moderate T2 hyperintensity	2.500	0.283, 22.088	0.410			
Corona enhancement	4.658	2.139, 10.143	**<0.001**	3.217	1.326, 7.861	**0.010**
Restricted diffusion	0.233	0.021, 2.643	0.240			
Fat sparing in solid mass	1.969	0.663, 5.842	0.222			
Iron sparing in solid mass	1.036	0.091, 11.747	0.977			

(*Continued*)

Table 3 (Continued).

Characteristic	Univariate Analysis			Multivariate Analysis		
	OR	95% CI	p value	OR	95% CI	p value
Non-LIRADS imaging features						
Non-smooth tumor margin	3.421	1.596, 7.333	**0.002**			
Internal arteries	6.125	2.647, 14.170	**<0.001**	4.147	1.596, 10.880	**0.004**
Peritumoral hypointensity on HBP	8.193	3.550, 18.908	**<0.001**	5.165	2.064, 12.923	**<0.001**

Note: p < 0.05 was defined as statistical significance (bold).
Abbreviations: HCC, hepatocellular carcinoma; LIRADS, The Liver Imaging Reporting and Data System; HBP, hepatobiliary phase; CI, confidence interval; OR, odds ratio.

recurrence in patients with LR-5 HCC. Multivariate Cox regression analysis demonstrated that mosaic architecture (hazard ratio [HR]=1.982; 95% CI: 1.147, 3.427; p = 0.014), corona enhancement (HR = 1.783; 95% CI: 1.031, 3.082; p = 0.0391), and peritumoral hypointensity on HBP (HR = 2.130; 95% CI: 2.130; p = 0.009) were independent risk factors associated with recurrence (Figure 2). The detailed results of univariate and multivariate regression analyses were summarized in Table 4.

Diagnostic Performance of Predictive Factors

The sensitivity, specificity, accuracy, positive predictive value, and negative predictive value for MVI prediction and RFS were summarized in Table 5. The area under the curve (AUC) for predicting MVI was 0.807 (95% CI: 0.725, 0.899), and the C-index for predicting recurrence was 0.725 (95% CI: 0.664, 0.786). Representative images of MVI and recurrence are shown in Figures 3 and 4.

Discussion

Considering that LR-5 HCC does not require postoperative histological confirmation, preoperative prediction of MVI and recurrence for LR-5 HCC patients can better assist clinicians in making individualized treatment options and follow-up plans. The current study aimed to identify the risk factors associated with MVI and recurrence in patients with LR-5 HCC. Our findings indicate that corona enhancement, internal arteries, and peritumoral hypointensity on HBP are independent predictors of MVI in patients with LR-5 HCC. Additionally, mosaic architecture, corona enhancement, and peritumoral hypointensity on HBP are prognostic factors associated with recurrence in patients with LR-5 HCC. These results provide valuable information for clinical decision-making and individualized treatment planning for patients with LR-5 HCC.

As an essential ancillary feature, corona enhancement is defined as an area of irregular hyperdensity immediately surrounding the tumor in the arterial phase that gradually became isointense in the venous and delayed phases. In the present study, we observed that corona enhancement is a significant predictor of MVI in patients with LR-5 HCC, complies with previous reports.[19,20] Research suggested that corona enhancement indicated the drainage of contrast agent from the HCC tumor into the peritumoral parenchyma, indicating vascular invasion and intrahepatic metastases.[20,21] Therefore, a recent review[22] considered corona enhancement to be an aggressive feature associated with HCC biological behavior. Additionally, Sheng et al[23] found that corona enhancement was an independent predictor of early recurrence - related outcome after TACE treatment for HCC. Similarly, our study demonstrated that patients with corona enhancement have worse RFS compared to those without this finding, which is similar to previous research.[24]

Peritumoral hypointensity on HBP may be caused by impaired function of organic anion-transporting polypeptide transporter proteins in hepatocytes around the tumor caused by altered hepatocyte perfusion around the HCC.[24] Our study highlighted the significant predictive value of this phenomenon for MVI in patients with LR-5 HCC. Prior research has also delved into the relationship between peritumoral hypointensity on HBP and MVI in HCC patients.[25–27] This connection can be explained by the fact that tumor cells in MVI-positive patients can lead to dysfunction of OATP transporter proteins in the hepatocytes of the peritumoral liver parenchyma, resulting in the observed peritumoral hypointensity on HBP.[28] Furthermore, our study confirmed that peritumoral hypointensity on HBP serves as an

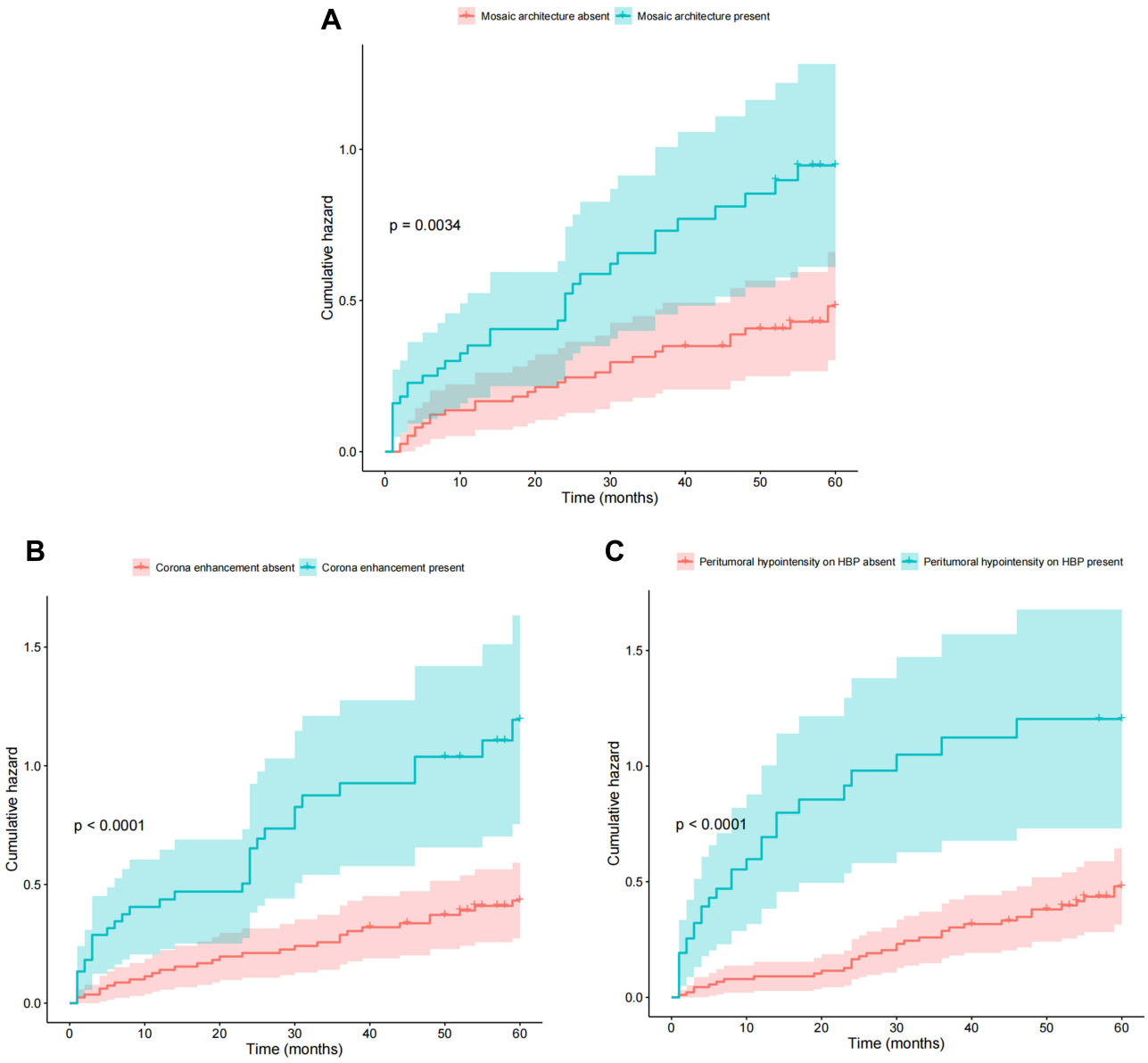

Figure 2 Kaplan–Meier curves of imaging features for RFS in LR-5 HCCs. (**A**) Mosaic architecture (absent) and Mosaic architecture (present) (Log rank test, p =0.034). (**B**) Corona enhancement (absent) and Corona enhancement (present) (Log rank test, p <0.0001). (**C**) Peritumoral hypointensity on HBP (absent) and Peritumoral hypointensity on HBP (present) (Log rank test, p <0.0001).

independent risk factor for predicting postoperative RFS in patients with LR-5 HCC, which was in agreement with prior research findings.[24,28] Notably, our investigation also revealed that peritumoral hypointensity on HBP exhibits high diagnostic accuracy for predicting MVI and recurrence. Therefore, determining the preoperative peritumor signal status on HBP appears to hold significant prognostic value and may inform more personalized HCC treatment strategies.

Internal arteries, while not a primary component of LIRADS, have been observed more frequently in studies of hepatocellular carcinoma.[29–31] The detection of internal arteries is a significant imaging feature in the evaluation of HCC, with a diagnostic specificity as high as 98% for HCC diagnosis.[32] Researchers have suggested that internal arteries were associated with poorly differentiated tumor cells, increased tumor proliferation, angiogenesis, and stromal invasion.[33] In the present study, we found that internal arteries were more prevalent in patients with MVI-positive HCC, which is consistent with previous findings.[30,31]

Mosaic architecture, as seen in imaging manifestation, is characterized by randomly distributed nodules or components within the tumor that exhibit different features in terms of density, attenuation, enhancement, morphology, and

Table 4 Univariate and Multivariate Cox Analyses for Recurrence with Patients of LR-5 HCC

Characteristic	Univariate Analysis			Multivariate Analysis		
	HR	95% CI	p value	HR	95% CI	p value
Tumor size >5cm	1.831	1.087, 3.083	**0.023**			
Multiple tumors	2.587	1.144, 5.849	**0.022**			
LI-RADS major features						
Non-rim arterial phase hyperenhancement						
Non-peripheral washout	0.656	0.238, 1.808	0.415			
Enhancing capsule	1.213	0.712, 2.067	0.477			
LI-RADS ancillary features (favoring HCC in particular)						
Non-enhancing capsule	1.109	0.528, 2.331	0.785			
Nodule-in-nodule architecture	2.021	1.113, 3.670	**0.021**			
Mosaic architecture	3.042	1.841, 5.026	**<0.001**	1.982	1.147, 3.427	**0.014**
Fat in mass, more than adjacent liver	1.036	0.562, 1.911	0.909			
Blood products in mass	0.784	0.373, 1.649	0.521			
LI-RADS ancillary features (favoring malignancy, not HCC in particular)						
Hepatobiliary phase hypointensity	0.709	0.430, 1.168	0.177			
Mild-moderate T2 hyperintensity	1.714	0.419, 7.013	0.454			
Corona enhancement	2.816	1.705, 4.652	**<0.001**	1.783	1.031, 3.082	**0.039**
Restricted diffusion	1.949	0.270, 14.069	0.508			
Fat sparing in solid mass	0.443	0.161, 1.220	0.115			
Iron sparing in solid mass	1.789	0.437, 7.324	0.419			
Non-LIRADS imaging features						
Non-smooth tumor margin	1.487	0.900, 2.458	0.121			
Internal arteries	1.727	1.020, 2.923	**0.042**			
Peritumoral hypointensity on HBP	3.492	2.108, 5.786	**<0.001**	2.130	1.208, 3.755	**0.009**

Note: p < 0.05 was defined as statistical significance (bold).
Abbreviations: HCC, hepatocellular carcinoma; LIRADS, The Liver Imaging Reporting and Data System; HBP, hepatobiliary phase; CI, confidence interval; HR, hazard ratios.

Table 5 Diagnostic Performance for Predicting MVI and Recurrence

MRI Findings	Sensitivity (%)	Specificity (%)	Accuracy (%)	PPV (%)	NPV (%)
Prediction of MVI					
Corona enhancement	60.5 (26/43)	75.3 (67/89)	70.5 (93/132)	54.2 (26/48)	79.8 (67/84)
Internal arteries	51.2 (22/43)	85.4 (76/89)	74.2 (98/132)	62.9 (22/35)	78.4 (76/97)
Peritumoral hypointensity on HBP	60.5 (26/43)	84.3 (75/89)	76.5 (101/132)	65 (26/40)	81.5 (75/92)
Prediction of recurrence					
Mosaic architecture	53.2 (33/62)	70 (49/70)	62.1 (82/132)	61.1 (33/54)	62.8 (49/78)
Corona enhancement	53.2 (33/62)	78.6 (55/70)	66.7 (88/132)	68.8 (33/48)	65.5 (55/84)
Peritumoral hypointensity on HBP	45.2 (28/62)	82.9 (58/70)	65.2 (86/132)	70 (28/40)	63.0 (58/92)

Abbreviations: MVI, microvascular invasion; HBP, hepatobiliary phase.

size.[34] Pathologically, mosaic architecture corresponds to different foci of clonal amplification in different stages of hepatocellular carcinoma, containing various intervals of fatty, necrotic, cystic, hemorrhagic, and fibrotic tissue.[35] This may reflect histological differences and tumor heterogeneity, explaining why the presence of mosaic structures serves as a risk factor for poor prognosis in HCC treatment. Previous studies have established mosaic architecture as a risk factor for TACE[23,36] and postoperative[17,37,38] recurrence in HCC patients. In agreement with these findings, our study also observed that HCC patients with mosaic structures had worse postoperative prognosis.

In contrast to previous studies in HCC populations,[23,37] we did not identify high AFP levels as an independent predictor of MVI and recurrence in patients with LR-5 HCC, which is similar to recent study for LR-5 HCC patients.[39]

Figure 3 Images of a 54-year-old man with chronic hepatitis B infection, categorized as LR-5 HCC with MVI and recurrence. (**A**) Heterogeneous mass with mosaic architecture on T2WI; (**B**) Non-rim arterial phase hyperenhancement (APHE) on the arterial phase, with corona enhancement and internal arteries (white arrow). (**C**) Peritumoral hypointensity (white arrow) in the hepatobiliary phase.

The potential reason for the discrepancies among these studies may include selection bias in the study population or differences in sample size.

Our study has several limitations. Firstly, selection bias is inevitable due to the retrospective study design and the exclusion of non-LR-5 HCC patients. While LR-4 and LR-M may also represent pathologically confirmed HCC, LR-5 is currently the most common type of HCC that does not require histopathological confirmation and is suitable for preoperative MRI evaluation. Secondly, the study population was selected based on LI-RADS criteria, limiting the generalizability of our findings to other regions with different liver diseases. Thirdly, the present study did not document threshold growth (a major feature of LI-RADS 5) due to the lack of reliance on multiple examination outcome. Finally, the follow-up period in this study was not long enough to accurately assess overall survival rates. Therefore, a prospective, multicenter study with a longer follow-up period is needed to evaluate the predictive value of Gd-BOPTA enhanced MRI imaging features for MVI, RFS, and OS in HCC patients.

In conclusion, corona enhancement, internal arteries, and peritumoral hypointensity on HBP were significantly associated with MVI in patients with LR-5 HCC. Furthermore, mosaic architecture, corona enhancement, and

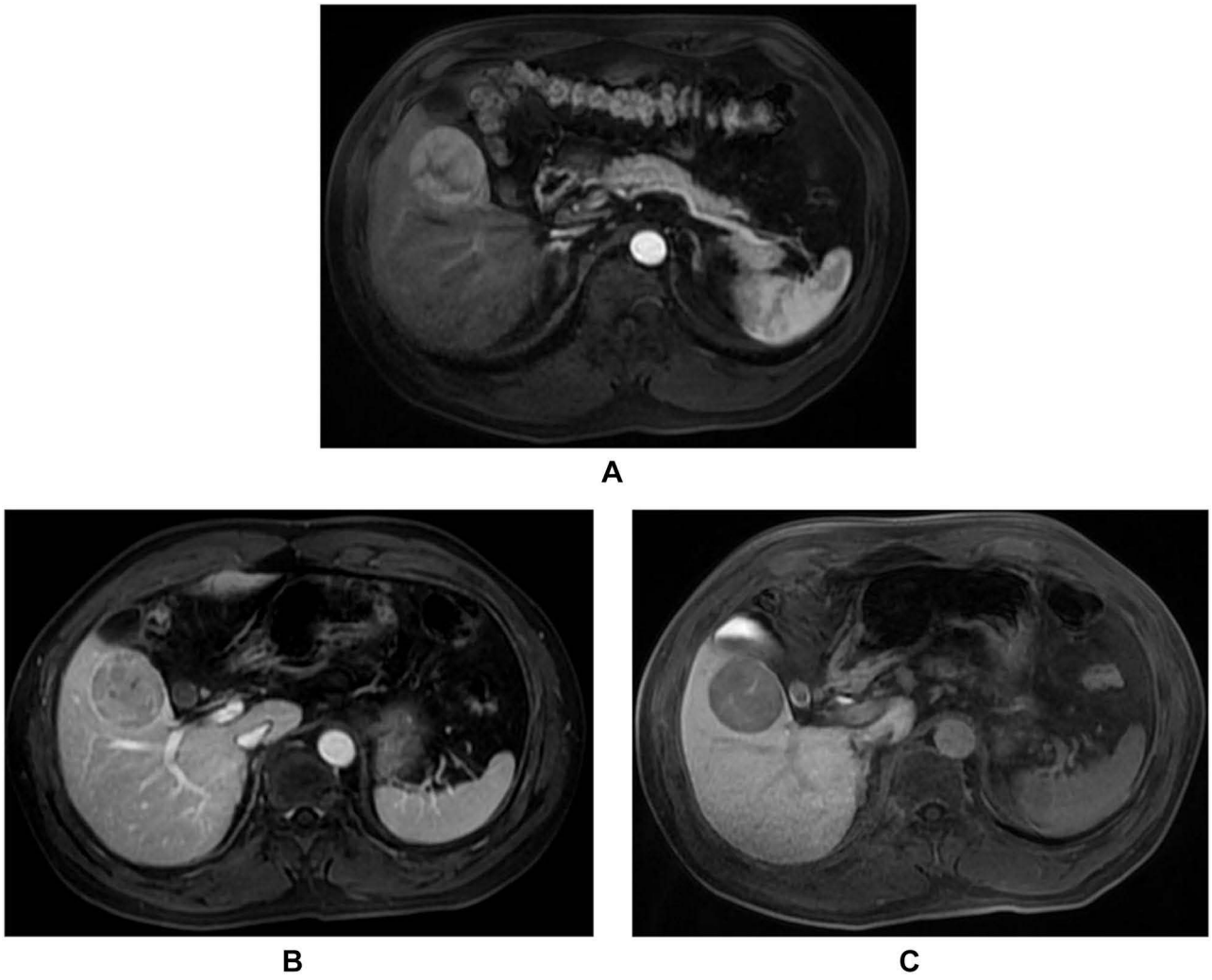

Figure 4 MR images of a 48-year-old man with chronic hepatitis B infection, categorized as LR-5 HCC without MVI and non-recurrence. (**A**) Non-rim arterial phase hyperenhancement (APHE) on the arterial phase. (**B**) Non-peripheral washout on the portal venous phase. (**C**) The lesion of hypointense on the HBP image.

peritumoral hypointensity on HBP were independent risk factors for postoperative RFS in patients with LR-5 HCC. Therefore, individualized treatment options should be implemented for patients at high risk of MVI in LR-5 HCC, as well as more frequent postoperative follow-up and adjuvant therapy for patients at high risk of RFS to improve survival time.

Disclosure

The authors report no conflicts of interest in this work.

References

1. Bray F, Ferlay J, Soerjomataram I, et al. Global cancer statistics 2018: GLOBOCAN estimates of incidence and mortality worldwide for 36 cancers in 185 countries. *CA Cancer J Clin*. 2018;68(6):394–424. doi:10.3322/caac.21492
2. Marrero JA, Kulik LM, Sirlin CB, et al. Diagnosis, staging, and management of hepatocellular carcinoma: 2018 practice guidance by the American Association for the Study of Liver Diseases. *Hepatology*. 2018;68(2):723–750. doi:10.1002/hep.29913
3. Hanazaki K, Kajikawa S, Shimozawa N, et al. Hepatic resection for large hepatocellular carcinoma. *Am J Surg*. 2001;181(4):347–353. doi:10.1016/s0002-9610(01)00584-0
4. Lin WP, Xing KL, Fu JC, et al. Development and validation of a model including distinct vascular patterns to estimate survival in hepatocellular carcinoma. *JAMA Network Open*. 2021;4(9):e2125055. doi:10.1001/jamanetworkopen.2021.25055
5. Yao LQ, Chen ZL, Feng ZH, et al. Clinical features of recurrence after hepatic resection for early-stage hepatocellular carcinoma and long-term survival outcomes of patients with recurrence: a multi-institutional analysis. *Ann Surg Oncol*. 2022;29(8):5206. doi:10.1245/s10434-022-11454-y

6. Chan AWH, Zhong J, Berhane S, et al. Development of pre and post-operative models to predict early recurrence of hepatocellular carcinoma after surgical resection. *J Hepatol*. 2018;69(6):1284–1293. doi:10.1016/j.jhep.2018.08.027
7. Lee S, Kim SH, Lee JE, et al. Preoperative gadoxetic acid-enhanced MRI for predicting microvascular invasion in patients with single hepatocellular carcinoma. *J Hepatol*. 2017;67(3):526–534. doi:10.1016/j.jhep.2017.04.024
8. Famularo S, Piardi T, Molfino S, et al. Factors affecting local and intra hepatic distant recurrence after surgery for Hcc: an alternative perspective on microvascular invasion and satellitosis - a Western European Multicentre Study. *J Gastrointest Surg*. 2021;25(1):104–111. doi:10.1007/s11605-019-04503-7
9. Kim AY, Sinn DH, Jeong WK, et al. Hepatobiliary MRI as novel selection criteria in liver transplantation for hepatocellular carcinoma. *J Hepatol*. 2018;68(6):1144–1152. doi:10.1016/j.jhep.2018.01.024
10. Ariizumi S, Kitagawa K, Kotera Y, et al. A non-smooth tumor margin in the hepatobiliary phase of gadoxetic acid disodium (Gd-EOB-DTPA)-enhanced magnetic resonance imaging predicts microscopic portal vein invasion, intrahepatic metastasis, and early recurrence after hepatectomy in patients with hepatocellular carcinoma. *J Hepatobiliary Pancreat Sci*. 2011;18(4):575–585. doi:10.1007/s00534-010-0369-y
11. Jiang H, Wei J, Fu F, et al. Predicting microvascular invasion in hepatocellular carcinoma: a dual-institution study on gadoxetate disodium-enhanced MRI. *Liver Int*. 2022;42(5):1158–1172. doi:10.1111/liv.15231
12. Rhee H, An C, Kim HY, et al. Hepatocellular carcinoma with irregular rim-like arterial phase hyperenhancement: more aggressive pathologic features. *Liver Cancer*. 2019;8(1):24–40. doi:10.1159/000488540
13. Zhang L, Yu X, Wei W, et al. Prediction of HCC microvascular invasion with gadobenate-enhanced MRI: correlation with pathology. *Eur Radiol*. 2020;30(10):5327–5336. doi:10.1007/s00330-020-06895-6
14. Kim H, Park MS, Choi JY, et al. Can microvessel invasion of hepatocellular carcinoma be predicted by pre-operative MRI? *Eur Radiol*. 2009;19(7):1744–1751. doi:10.1007/s00330-009-1331-8
15. Chernyak V, Fowler KJ, Kamaya A, et al. Liver Imaging Reporting and Data System (LI-RADS) version 2018: imaging of hepatocellular carcinoma in at-risk patients. *Radiology*. 2018;289(3):816–830. doi:10.1148/radiol.2018181494
16. Shin J, Lee S, Kim SS, et al. Characteristics and early recurrence of hepatocellular carcinomas categorized as LR-M: comparison with those categorized as LR-4 or 5. *J Magn Reson Imaging*. 2021;54(5):1446–1454. doi:10.1002/jmri.27650
17. Wang L, Feng B, Li D, et al. Risk stratification of solitary hepatocellular carcinoma ≤ 5 cm without microvascular invasion: prognostic values of MR imaging features based on LI-RADS and clinical parameters. *Eur Radiol*. 2023;33(5):3592–3603. doi:10.1007/s00330-023-09484-5
18. Kim KA, Kim MJ, Jeon HM, et al. Prediction of microvascular invasion of hepatocellular carcinoma: usefulness of peritumoral hypointensity seen on gadoxetate disodium-enhanced hepatobiliary phase images. *J Magn Reson Imaging*. 2012;35(3):629–634. doi:10.1002/jmri.22876
19. Zhu Y, Feng B, Cai W, et al. Prediction of microvascular invasion in solitary AFP-negative hepatocellular carcinoma ≤ 5 cm using a combination of imaging features and quantitative dual-layer spectral-detector CT parameters. *Acad Radiol*. 2023;30(Suppl 1):S104–S116. doi:10.1016/j.acra.2023.02.015
20. Liu HF, Zhang YZ, Wang Q, et al. A nomogram model integrating LI-RADS features and radiomics based on contrast-enhanced magnetic resonance imaging for predicting microvascular invasion in hepatocellular carcinoma falling the Milan criteria. *Transl Oncol*. 2023;27:101597. doi:10.1016/j.tranon.2022.101597
21. Kitao A, Zen Y, Matsui O, et al. Hepatocarcinogenesis: multistep changes of drainage vessels at CT during arterial portography and hepatic arteriography--radiologic-pathologic correlation. *Radiology*. 2009;252(2):605–614. doi:10.1148/radiol.2522081414
22. Kovac JD, Ivanovic A, Milovanovic T, et al. An overview of hepatocellular carcinoma with atypical enhancement pattern: spectrum of magnetic resonance imaging findings with pathologic correlation. *Radiol Oncol*. 2021;55(2):130–143. doi:10.2478/raon-2021-0004
23. Sheng Y, Wang Q, Liu HF, et al. Preoperative nomogram incorporating clinical factors, serological markers and LI-RADS MRI features to predict early recurrence of hepatocellular carcinoma treated with transarterial chemoembolization. *Acad Radiol*. 2023;30(7):1288–1297. doi:10.1016/j.acra.2022.10.020
24. Wei H, Jiang H, Zheng T, et al. LI-RADS category 5 hepatocellular carcinoma: preoperative gadoxetic acid-enhanced MRI for early recurrence risk stratification after curative resection. *Eur Radiol*. 2021;31(4):2289–2302. doi:10.1007/s00330-020-07303-9
25. Zhang K, Xie SS, Li WC, et al. Prediction of microvascular invasion in HCC by a scoring model combining Gd-EOB-DTPA MRI and biochemical indicators. *Eur Radiol*. 2022;32(6):4186–4197. doi:10.1007/s00330-021-08502-8
26. Zhang S, Huo L, Zhang J, et al. A preoperative model based on gadobenate-enhanced MRI for predicting microvascular invasion in hepatocellular carcinomas (≤ 5 cm). *Front Oncol*. 2022;12:992301. doi:10.3389/fonc.2022.992301
27. Hong SB, Choi SH, Kim SY, et al. MRI features for predicting microvascular invasion of hepatocellular carcinoma: a systematic review and meta-analysis. *Liver Cancer*. 2021;10(2):94–106. doi:10.1159/000513704
28. Chen Z, Li X, Zhang Y, et al. MRI features for predicting microvascular invasion and postoperative recurrence in hepatocellular carcinoma without peritumoral hypointensity. *J Hepatocell Carcinoma*. 2023;10:1595–1608. doi:10.2147/JHC.S422632
29. Tang Y, Lu X, Liu L, et al. A reliable and repeatable model for predicting microvascular invasion in patients with hepatocellular carcinoma. *Acad Radiol*. 2023;30(8):1521–1527. doi:10.1016/j.acra.2023.02.035
30. Zheng X, Xu YJ, Huang J, et al. Predictive value of radiomics analysis of enhanced CT for three-tiered microvascular invasion grading in hepatocellular carcinoma. *Med Phys*. 2023;50(10):6079–6095. doi:10.1002/mp.16597
31. Yang WL, Zhu F, Chen WX. Texture analysis of contrast-enhanced magnetic resonance imaging predicts microvascular invasion in hepatocellular carcinoma. *Eur J Radiol*. 2022;156:110528. doi:10.1016/j.ejrad.2022.110528
32. Nino-Murcia M, Olcott EW, Jeffrey RB, et al. Focal liver lesions: pattern-based classification scheme for enhancement at arterial phase CT. *Radiology*. 2000;215(3):746e51. doi:10.1148/radiology.215.3.r00jn03746
33. Segal E, Sirlin CB, Ooi C, et al. Decoding global gene expression programs in liver cancer by noninvasive imaging. *Nat Biotechnol*. 2007;25(6):675–680. doi:10.1038/nbt1306
34. Choi JY, Lee JM, Sirlin CB. CT and MR imaging diagnosis and staging of hepatocellular carcinoma: part II. Extracellular agents, hepatobiliary agents, and ancillary imaging features. *Radiology*. 2014;273(1):30–50. doi:10.1148/radiol.14132362
35. Cerny M, Chernyak V, Olivié D, et al. LI-RADS Version 2018 Ancillary Features at MRI. *Radiographics*. 2018;38(7):1973–2001. doi:10.1148/rg.2018180052

36. Bao Y, Li JX, Zhou P, et al. Identifying proliferative hepatocellular carcinoma at pretreatment CT: implications for therapeutic outcomes after transarterial chemoembolization. *Radiology*. 2023;308(2):e230457. doi:10.1148/radiol.230457
37. Wei H, Fu F, Jiang H, et al. Development and validation of the OSASH score to predict overall survival of hepatocellular carcinoma after surgical resection: a dual-institutional study. *Eur Radiol*. 2023;33(11):7631–7645. doi:10.1007/s00330-023-09725-7
38. Wei Y, Pei W, Qin Y, Su D, Liao H. Preoperative MR imaging for predicting early recurrence of solitary hepatocellular carcinoma without microvascular invasion. *Eur J Radiol*. 2021;138:109663. doi:10.1016/j.ejrad.2021.109663
39. Liang X, Shi S, Gao T. Preoperative gadoxetic acid-enhanced MRI predicts aggressive pathological features in LI-RADS category 5 hepatocellular carcinoma. *Clin Radiol*. 2022;77(9):708–716. doi:10.1016/j.crad.2022.05.018